The Solution Conformation of Polymer Brushes Determines their Interactions with DNA and Transfection Efficiency

Mahentha Krishnamoorthy[#,1,2] Danyang Li[#,1,2] Amir S. Sharili,[3] Tina Gulin-Sarfraz,[4] Jessica M. Rosenholm[4] and Julien E. Gautrot*[1,2]

[1]Institute of Bioengineering and [2]School of Engineering and Materials Science, Queen Mary, University of London, Mile End Road, London, E1 4NS, UK.

[3]Barts and the London School of Medicine and Dentistry, Queen Mary, University of London, 4 Newark Street, London, E1 2AT, UK.

[4]Pharmaceutical Sciences Laboratory, Faculty of Science and Engineering, Abo Akademi University, 20520 Turku, Finland.

[#] Both authors contributed equally to this work.

* To whom correspondence should be addressed, e-mail: j.gautrot@qmul.ac.uk.

1   **ABSTRACT**

2   Polymer brush-functionalised nanomaterials offer interesting features for the design of gene delivery

3   vectors as their physico-chemical and structural properties can be designed independently of the

4   chemistry, size and shape of the nanomaterial core. However, little is known of the parameters

5   regulating the adsorption and infiltration of DNA molecules at the surface of positively charged

6   polymer brushes, despite the importance of such processes for gene delivery. Here we investigate the

7   role of the molecular environment (e.g. pH, type of buffer, concentration) on the interactions between

8   plasmid DNA and positively charged poly(dimethylaminoethyl methacrylate) (PDMAEMA) brushes

9   using a combination of light scattering, electrophoretic light scattering, in situ ellipsometry and surface

10   plasmon resonance. We show that the conformation of swollen PDMAEMA brushes is modulated by

11   the surrounding buffer and that this impacts strongly on the ability of such brushes and nanomaterials

12   based on these coatings to complex DNA molecules. In turn, the levels of transfection efficiency

13   measured correlate with changes in brush conformation and DNA binding. Therefore, this work

14   demonstrates the importance of molecular design of polymer brushes to control DNA complexation

15   and potentially release in order to optimise the performance of polymer brush-functionalised

16   nanomaterials for gene delivery applications.

17

18

19

20

1 **INTRODUCTION**

2 Polymer brushes have attracted considerable interest in the fields of catalysis, sensing and biomedical

3 applications[1-4] as they allow the efficient and robust coating of surfaces without significantly altering

4 bulk properties of materials and can allow the control of the responsive and bioactive properties of

5 such interfaces. In the biomedical field, these coatings have found particular application in the

6 prevention of protein fouling and the design of biosensors, the generation of cell micropatterns for

7 cell-based assays and the control of bacterial adhesion and biofilm formation. However, relatively little

8 work has been carried out to investigate their use as drug delivery systems, perhaps because of the

9 limited loading levels they can typically achieve. In this respect, polymer brushes are well-adapted to

10 promote the complexation of DNA and control the delivery of such materials for gene transfection as

11 they can be designed to display cationic charges promoting DNA binding and gene delivery typically

12 requires moderate levels of biomacromolecule delivery to result in successful transfections. This was

13 demonstrated, for example, in the case of superparamagnetic iron oxide nanoparticles, which offer

14 the added opportunity to use magnetic sorting to further enrich cell populations displaying higher

15 expression levels of the corresponding plasmid[5, 6]. Hence, polymer brushes are interesting systems for

16 gene delivery approaches as they offer the control of several key structural and physico-chemical

17 parameters: the size and type of nanoparticles or nanomaterials, the density and length of polymer

18 chain coatings and the chemistry of the monomers used. However, relatively little is known of the

19 impact of these different parameters on DNA complexation and transfection efficiencies.

20 Gene delivery involves multiple stages, each impacted by a number of independent parameters,

21 making it a relatively difficult process to control and design[7, 8]. In the case of gene delivery mediated

22 by cationic polymeric vectors, these stages involve the initial complexation of DNA molecules by the

23 cationic polymers, the further maturation of the resulting complexes in the transfection medium, their

24 interaction with the cell membrane (and potentially receptors), their uptake (often via endocytosis),

25 release from the endosome, transportation to the perinuclear space, release of the DNA material and

26 translocation of nucleic acid molecules to the nucleus prior to their transcription[9, 10]. Such complexity

27 presumably explains the difficulty of rational design of DNA delivery vectors. In this context, polymer

28 brushes, and the control they offer over structural and physico-chemical properties, appear as

29 promising candidates to tackle some of the questions underlying such design.

30 Understanding the parameters controlling DNA-brush interactions is fundamental to vector design as

31 such interactions control the initial complexation of nucleic acid material as well as its release.

32 Although protein-brush interactions have been thoroughly studied in a number of cases (e.g. albumin,

33 fibronectin, enzymes), interactions of nucleic acid molecules with polymer brushes are less well

understood. Although such interactions are expected to be mediated by the electrostatic attraction between negatively charged phosphate groups and positive moieties on the polymer brush backbone, the impact of the controlled brush architecture, charge density and type (e.g. quaternary ammonium vs. protonated tertiary amines) on the binding and infiltration of DNA biomacromolecules into brushes is not known.

Poly(dimethylaminoethyl methacrylate) (PDMAEMA) is a polymer bearing tertiary amine side chains that display a pKa near 7.5 and become protonated and positively charged at neutral and low pH[11-13]. This polymer also displays a lower critical solution temperature, also dependent on pH[14]. As a result of its ease of synthesis, moderate cytotoxicity and positive charge at neutral pH, PDMAEMA has attracted some attention as a potential candidate for gene delivery applications[12]. Linear PDMAEMA was used to complex plasmid DNA and the resulting particles displayed reasonable transfection efficiencies[15]. In addition, the ability to grow PDMAEMA readily via controlled radical polymerisation techniques, in particular atom transfer radical polymerisation, has allowed the formation of a number of derivatives with more complex molecular architectures, ranging from diblock copolymers to multi-arm copolymers[16-19] and also displaying encouraging transfection levels. Recently, PDMAEMA polymer brushes grown from iron oxide superparamagnetic nanoparticles were also used to transfect CHO cells and L929 fibroblasts and sort out transfected cells in order to improve protein expression levels[20]. However, little is known of the parameters impacting on the performance of such PDMAEMA brushes-based nanoparticles on gene delivery and protein expression.

In this article, we investigate some of the parameters controlling gene delivery mediated by PDMAEMA-grafted nanoparticles, in particular the role of the molecular environment (pH, type of buffer, concentration), on interactions between DNA molecules and polymer brushes, and the resulting impact these have on gene transfection. We study the conformation of PDMAEMA and the level of plasmid DNA binding in different buffers and at different pH, using a combination of light scattering, electrophoretic light scattering, in situ ellipsometry and surface plasmon resonance. We investigate the cytotoxicity of the resulting particles and complexes, their uptake by the HaCaT epidermal cell line and their ability to promote gene transfection via fluorescence microscopy.

EXPERIMENTAL SECTION

Materials. 2-(Dimethylamino)ethyl methacrylate (DMAEMA, M_n = 157.21, copper chloride (Cu(I)Cl), copper bromide (Cu(II)Br$_2$), 2, 2'-bipyridyl (bpy), bromoisobutyryl bromide, (3-Aminopropyl)triethoxysilane, anhydrous toluene and triethylamine (Et$_3$N) were purchased from Sigma-Aldrich and used as received. All chemicals and solvents were analytical grades unless

otherwise stated. Cu(I)Cl was kept under vacuum until used. Deionised water, with resistivity of 18.2 MΩ·cm was obtained using Milli-Q Integral 3 System from Millipore. Silicon wafers (100 mm diameter, ⟨100⟩ orientation, polished on one side/reverse etched) were purchased from Compart Technology Ltd and cleaned in Plasma System Zepto from Diener Electronic, for 10 min in air plasma. Gold-coated silicon wafers were obtained through the evaporation of a chromium layer (20 nm followed by the evaporation of a gold layer (200 nm) using an Edwards Auto 500 evaporator. Silica particles (unfunctionalised) were purchased from Bangs Laboratories (supplied as powder, mean diameters of 310 nm). The size of these particles was confirmed by SEM (330 ± 10 nm) and light scattering (347 ± 21 nm). These particles were selected based on the reproducibility and good monodisperse character, as well as their ease of functionalisation with ATRP initiator silanes. The thiol ester initiator, ω-Mercaptoundecylbromoisobutyrate, **1** was synthesised as described in the literature[21], and the ester silane initiator, trimethoxy-3-propylbromoisobutyrate silane **2** was synthesised according to reported protocoles[22, 23]. For DNA interactions studies: NaCl (150 mM, PolyPlus), PBS (tablets, Sigma-Aldrich), KSFM (Gibco), HEPES-buffered saline (HBS, 1 M, Gibco), 10 x 12 mm SPR-Au chips purchased from Senss bv, and stored under nitrogen, at room temperature). 10 mM HBS contained 1mL of 1 M HEPES and 100 mL of 150 mM NaCl. Enhanced Green Fluorescent Protein (EGFP) prepared by Dr Julien Gautrot and Dr Amir Sharili. For cell culture: Versene (Gibco), Trypsin (0.25%, Gibco), Dulbecco's Modified Eagle Medium (DMEM, Gibco), DMEM-F12 (Gibco), L-Glutamine (200 mM, Gibco), Penicillin Streptomycin (PS, 5000 U/mL, Gibco), keratinocyte serum free medium (KSFM, Gibco) were purchased from Life Technologies. Collagen (rat, type I, BD Sciences, San Jose, CA), foetal bovine serum (FBS, LabTech) and sterile Dulbecco's Phosphate Buffered Solution (DPBS, PAA Laboratories/ Sigma-Aldrich) were also used. KSFM supplemented with 1 mL pituitary extract (Gibco), 3 μL EGF human recombinant (Gibco) and 5 mL PS, FAD medium prepared with 100 mL DMEM, 100 mL DMEM-F12, 20 mL FBS, 2.2 mL PS, hydrocortisone (0.5 μg/mL) containing 10-10 M cholera toxin, 10 ng/mL EGF and insulin (5 mg/mL), and DMEM medium supplemented with 50 mL bovine serum, 5 mL L-glutamine and 5 mL PS were used for the culture of primary keratinocytes and fibroblasts, respectively. 4',6-Diamidino-2-phenylindole dihydrochloride (DAPI, Sigma), 4% paraformaldehyde (PFA) prepared from 16g PFA (Sigma Aldrich) and PBS (Sigma-Aldrich) dissolved in deionised water, 0.2% Triton X-100 prepared from Triton X-100 (Sigma Aldrich) and PBS were used for immunostaining. EGFP was used for cell transfection. LIVE/DEAD® Viability/Cytotoxicity Kit containing 4 mM calcein AM in anhydrous DMSO and 2 mM ethidium homodimer in DMSO/H2O 1:4 (v/v), for mammalian cells was purchased from Life Technologies. Deionised water with a resistivity of 18.2 MΩ·cm was obtained using a purification system from Millipore.

1 **Methods.**

2 *ATRP initiator deposition.* For the deposition of thiol initiator on gold-coated silicon wafers:

3 gold-coated silicon substrates were immersed in 5 mM ethanolic solutions of the thiol initiator, and

4 left at room temperature overnight, in a sealed glass vial. The substrates were then washed in copious

5 amounts of ethanol and dried under a stream of nitrogen. For the deposition of ester silane initiator

6 on silicon wafers: plasma-oxidised silicon wafers were immersed in a recrystallisation dish containing

7 dry toluene (30 mL), Et_3N (50 µL) and silane initiator (10 µL), and covered with aluminium foil and left

8 at room temperature overnight. The wafers were then washed with ethanol and dried under a stream

9 of nitrogen. The initiator functionalised wafers were kept under nitrogen until used. For the

10 immobilization of ATRP initiator on silica nanoparticles: silica nanoparticles (D ≈ 310 nm, 200 mg) were

11 dispersed in dry toluene in a 15 mL centrifuge tube by sonication (Ultrawave IND7800D Ultrasonic

12 Cleaning Tank), washed in dry toluene via three centrifugation (4000 rpm for 1 minute)/ redispersion

13 cycles, and finally dispersed in dry toluene (4 mL). Triethylamine (200 µL) and silane initiator 2 (40 µL)

14 were added to this dispersion and the suspension was left on a 3D lab application shaker (Gyro Twister

15 GX-1000 3-D Shaker from Labnet), with the centrifuge tube placed on its side overnight for thorough

16 mixing. The resulting particles were collected by centrifugation, washed three times with dry toluene,

17 and finally redispersed in 4 mL ethanol as stock solution for storage (50 mg/mL).

18 *PDMAEMA brush growth on gold and silicon substrates.* A solution of $CuBr_2$ (18 mg, 80 µmol), bpy (320

19 mg, 2.05 mmol), and DMAEMA (6.6 g, 42 mmol) in water/ethanol (4/1 v/v, 30 mL) was degassed using

20 nitrogen bubbling for 20 min in a round-bottom flask with a stopper. Pre-weighed CuCl (82 mg, 828

21 µmol) was added to this solution and the resulting mixture was further degassed for 20 min. A glass

22 syringe was used to transfer 2 mL of the polymerisation solution to tubes containing the initiator-

23 coated surfaces under inert atmosphere whilst ensuring that the substrates are completely immersed

24 in the solution. The polymerisation was stopped at 5 or 20 min to obtain thicknesses of 10 nm and 30

25 nm respectively, by immersing the coated substrates in deionised water, followed by washing with

26 copious amounts of ethanol and drying in a nitrogen stream.

27 *Synthesis of PDMAEMA brush from silica nanoparticles.* Polymerisation solutions were prepared as

28 described previously by dissolving pre-weighed bpy (320 mg, 2.05 mmol) and $CuBr_2$ (18 mg, 80 µmol)

29 in DMAEMA (6.6 g, 42 mmol) and half of the total polymerisation solvent (water/ethanol 4/1 v/v, 15

30 mL) in a round-bottom flask. This was followed by the addition of pre-weighed CuCl (82 mg, 828 µmol)

31 and further stirring.. Initiator-coated silica nanoparticles (1/10 v/v, 100 µL, 50 mg/mL stock solution in

1 ethanol) were diluted in ethanol (1/10 v/v, 100 μL) and water (8/10 v/v, 800 μL) in a tube and degassed

2 in nitrogen/argon for 15 min. The polymerisation solution was then injected using a glass syringe into

3 the initiator-coated silica nanoparticles and left at room temperature whilst under inert atmosphere,

4 for 20 min. To terminate the polymerisation, the dispersion was diluted with water, and compressed

5 air was bubbled through the mixture until a colour change of dark brown to blue-green was observed.

6 The nanoparticles were recovered by centrifugation, washed three times with water and finally

7 dispersed in water.

8 *Synthesis of fluorescently-labelled, PDMAEMA-coated silica nanoparticles for characterisation of*

9 *cellular uptake.* Fluorescent mesoporous silica nanoparticles (F-MSNs) were synthesized according to

10 our previously published protocols[24], where methanol was used as co-solvent and

11 cetyltrimethylammoniumchloride (CTAC) as a structure-directing agent. In brief, 1.19 g of

12 tetramethoxysilane (TMOS) was mixed with aminopropyltrimethoxysilane (APTMS) and fluorescein

13 isothiocyanate (FITC) to create inherently fluorescent particles; and added dropwise to an alkaline

14 solution containing CTAC. The resulting synthesis mixture had a molar ratio of 0.9 TMOS: 0.1 APTMS:

15 1.27 CTAC: 0.26 NaOH: 1439 MeOH: 2560 H_2O. The mixture was stirred overnight at room

16 temperature, whereafter the formed particles were separated by centrifugation, washed with

17 deionized water and vacuum dried for 24 h. The CTAC template was then removed by ultrasonication

18 of the particles in acidic (HCl) ethanol three times. Particles were subsequently functionalised with

19 polymer brushes, as described above, after initiator immobilisation.

20 **Characterisation.**

21 *Thermogravimmetric analysis.*The weight percent (wt%) of polymer coating on silica nanoparticles

22 was determined by TGA. Measurements were performed in air using TA Instruments Q500. Samples

23 were heated from room temperature to 1000 °C at a heating rate of 10 °C/min and dried under

24 vacuum at room temperature prior to TGA runs. It was assumed that the mass change was due to the

25 burning of the organic polymer brush coatings and the remainder was non-combustible silica particles.

26 According to TGA results, the PDMAEMA dry thickness on silica nanoparticle can be calculated using

27 equation S1 (Supplementary Information).

28 *Dynamic light scattering and electrophoretic light scattering.* Interactions of DNA with the silica

29 nanoparticles coated with PDMAEMA brushes were carried out with Zetasizer Nano ZS. Plasmid DNA

30 (4400 bp) was dissolved in the concentration of 10 μg/mL and diluted in 1 mL of 150 mM NaCl. Polymer

31 brush-coated nanoparticles were also diluted in 1 mL of 150 mM NaCl for the N/P ratios 1:1, 5:1 and

1   20:1, where N/P ratio is the ratios of moles of the amine groups of cationic polymers to those of the

2   phosphates from DNA. The amount of DNA used was kept constant here whilst the amount of the

3   polymer brush-coated nanoparticles was varied. 1 mL of the polymer brush-grafted nanoparticles

4   solution was added to 1mL of the DNA solution and allowed to complex for 15-30 min. The particle

5   hydrodynamic diameter and the zeta potential were then measured for each N/P ratio before and

6   after complexation. The hydrodynamic diameter of nanoparticles in different buffers (in the absence

7   of DNA) was characterised with 20 μg/mL particle solutions (at higher concentrations, some level of

8   aggregation was observed). It should be noted that, given the size of the particles used and the

9   wavelength of the laser used (633 nm), multiple scattering is also expected to occur and may have an

10 impact on the accurate measurements of particle sizes, depending on concentration.

11 *Surface Plasmon Resonance.* SPR measurements were performed with a Biacore X using 10 and 30

12 nm-thick PDMAEMA brushes. Plasmid DNA (EGFP, 4400 bp) dissolved in the concentration of 1 μg/mL

13 in 150 mM NaCl, 10 mM HBS buffer or PBS, at pH 7.4, was allowed to interact with the immobilised

14 polymer brush. Saline solution (150 mM NaCl) at pH 9 and pH 5 were also injected to study binding

15 stability at different pH.

16 *Ellipsometry.* The dry polymer film thickness measurements were obtained via an α-SE spectroscopic

17 ellipsometer (J. A. Woollam) at an incident angle of 70°. Bare substrates of silicon was used to build

18 the model using a cauchy layer to measure the brush thickness. Silicon wafers (1 cm x 3 cm) grafted

19 with PDMAEMA were measured at three different points per sample and average values were

20 reported ± standard deviations. For *in situ* measurements, the wafers were mounted on the liquid cell,

21 and injected with 10 mM HBS/150 mM NaCl buffer and allowed to reach its swelling equilibrium. This

22 was then followed by injection of plasmid DNA dissolved in the respective buffer, and the wet

23 thickness was measured at regular intervals.

24 *In vitro cell viability assay.* The cell viability of PDMAEMA-coated silica particles was evaluated on

25 HaCaT cells by using live/dead assay. HaCaT cells were cultured in Dulbecco's Modified Eagles Medium

26 (DMEM) with 10 % fetal bovine serum (FBS), 1% penicillin/streptomycin and 1% glutamine, then cells

27 were maintained in a humidified atmosphere of 5% CO_2 at 37℃ with the medium changed every other

28 day. Two 24-well plates were coated with 20 μg/mL collagen diluted in DPBS per well, for 30 min at

29 RT, and washed with DPBS before being seeded with HaCaTs at a density of 25k cells per well (500 μL).

30 Live/dead assay was carried out at 4 h and 24 h time points. Prior to seeding, the medium was replaced

31 from each well with 500 μL KSFM without supplements on the following day. Cells were either

incubated with particle suspensions only or particle suspensions with DNA in the N/P ratios 1:1, 3:1, 5:1, 7:1, 10:1 and 20:1. A well was left without exposure to nanoparticles or DNA as a positive control. 50 µL of 150 mM NaCl containing 1 µg of EGFP plasmid (i.e 2.8 µL of 0.358 µg/µL EGFP stock solution) was added to 50 µL of 150 mM NaCl containing PDMAEMA-coated particles (3.8 mg/mL stock solution concentration) of the required N/P ratios (N/P 1:1 = 1.3 µL, 3:1= 3.9 µL, 5:1=6.5 µL, 7:1=9.1 µL, 10:1=13 µL, 20:1=26 µL). These were incubated for 15 min at room temperature. 100 µL of each complex was added dropwise into a row of wells (24-well plate) containing the cells as prepared above. In addition, 100 µL of 150 mM NaCl containing PDMAEMA-coated particles (3.8 mg/mL) were then added dropwise into another row of the 24-well plate in which cells had been seeded as above. After 4 h or 24 h, the medium in the well was replaced with 1 mL DMEM containing 4 mM calcein AM (0.5 µL) and 2 mM ethidium homodimer (2 µL). The well-plate was incubated for 30 min at 37°C, and imaged using a Leica DMI4000B Epifluorescent Microscope after 4 h or after 24 h.

In vitro transfection assays. The protocol for the transfections with PDMAEMA was adapted from jetPEI® *in vitro* DNA Transfection Protocol from PolyPlus transfection™. 2 µL of jetPEI® per µg of DNA was used as a control, following a protocol recommended by the manufacturer, with minor changes to conditions for optimisation of transfection efficiencies (DNA concentration, cell density, time of incubation) with our cell culture system. For transfection with polymer brushes, 1 µg of DNA, 2 µL of jetPEI® reagent and PDMAEMA-g-SiO$_2$ at N/P ratios 5:1, 10:1 and 15:1 were diluted in 50 µL of 150 mM NaCl solution separately. 50 µL of the resulting cationic polymer solution was then added to the 50 µL DNA solution (adding in the reversed order can reduce transfection efficiency), the resulting solution was mixed gently and then incubated for 15 to 30 min at room temperature. 100 µL of the cationic polymer/DNA mix was then added dropwise to each well containing the cells seeded on the previous day (density: 25k) in 1 mL of KSFM and gently mixed by moving the plate side-to-side. The complexes were incubated with the cells for 4 hours then the medium was replaced with KSFM with supplements. The cells were incubated for a further 24 h to allow sufficient expression of the plasmid DNA before performing reporter gene assay.

Fluorescence imaging. Transfection efficiencies were measured from counting the number of transfected cells expressing EGFP and the total number of cells, stained with 4',6-Diamidino-2-phenylindole dihydrochloride (DAPI). Quantification was carried out using ImageJ. Following thresholding of the DAPI channel of images, individual nuclei were recognised automatically by ImageJ using the 'Analyze Particles' function (with a size threshold of 50 pixels). Corresponding intensities measured in the EGFP channels were automatically measured for each nuclei. EGFP positive cells were defined with a threshold two-fold higher than the basal fluorescence level (defined as the fluorescence

1 level of the lowest 5% cells). The number of transfected cells as a percentage of the total number of

2 cells was then presented in all studies involving transfection efficiency.

3 Confocal laser scanning microscopy (CLSM) was used to observe the subcellular distribution of

4 particles after incubation. Three-dimensional images of HaCaT cells, with Δz = 300 nm were acquired

5 via CLSM. The main panel from the CLSM image shows the fluorescent image in the x-y cross-section

6 at a given z-location whilst the 2 smaller panels show the structure along the x-z (bottom) and y-z

7 (right side panel) at the position indicated by the yellow lines in the main panel (as in Figure 4B).

8 *Statistical analysis.* The statistical analysis was performed for the cell viability and transfection results

9 via one-way ANOVA followed by Tukey's test using OriginPro 9.0 and pairwise Student's T-test for post

10 hoc analysis where p values < 0.05 were considered significant (* = $p<0.05$, ** = $p < 0.01$ and *** = p

11 < 0.001). All data values are expressed as mean ± standard error (SE) where $n \geq 3$.

12 *Determination of brush grafting density on silica nanoparticles.* The grafting density of PDMAEMA

13 brushes grown from silica nanoparticles was determined using equation S2, taking into account the

14 weight percentage (characterised by TGA) and molecular weight of PDMAEMA brushes grown from

15 silica nanoparticles. For characterization of the molecular weight, PDMAEMA brushes were cleaved

16 from silica nanoparticles and characterized via gel permeation chromatography (GPC). Briefly, 5 mL

17 SiO_2-PDMAEMA particle suspension (20 mg/mL) was added to 25 mL 10 % hydrofluoric acid solution

18 and stirred at room temperature for 4 h. The cloudy particle suspension turned clear after the silica

19 core dissolved completely. The solution was then transferred to a 3.5 KD Spectra/Por® dialysis bag,

20 dialysed with deionised water and freeze dried afterwards. GPC measurements were carried on an

21 Agilent 1260 infinity system operating in dimethylformamide (DMF) with 5 mM ammonium

22 tetrafluoroborate at 50 °C and equipped with refractive index detectors and variable wavelength

23 detectors. The instrument was calibrated with linear narrow polystyrene standards in a range of 550

24 to 46,890 g/mol. 2 mg of PDMAEMA cleaved from silica nanoparticles was fully dissolved in 2 mL of

25 DMF and filtered before GPC characterization.

26 **RESULTS AND DISCUSSION**

27 **Synthesis of PDMAEMA-grafted particles.** PDMAEMA brushes were grown from silica nanoparticles

28 functionalised with ATRP initiator molecules, using modified protocols reported in the literature

29 (Figure 1)[25, 26]. Targeted thicknesses were 10 and 30 nm, and corresponding polymerisation times were

30 determined from the kinetics of PDMAEMA brush growth from silicon wafers (Supplementary Figure

31 S1, in Supplementary Information). The hydrodynamic size of the corresponding silica nanoparticles

1   and their zeta potential ζ were 650 nm and 40.0 mV (for 30 nm brushes) in deionised water, as

2   determined via dynamic light scattering (DLS) and electrophoretic light scattering. These values are

3   consistent with the size of the dry brushes generated and their expected positive charge at neutral pH

4   (similar to high levels of swelling reported for positively charged PMETAC and PDEA brushes grown

5   from nanoparticles[25,27, 28]). TGA confirmed the formation of a polymer shell surrounding nanoparticles

6   (Supplementary Figure S2). It is clear that the weight loss occurs in two stages. The first weight loss

7   from RT to 200 °C, with a more pronounced decrease below 100 °C, is caused by the desorption of

8   physically adsorbed water. The second stage, which takes place above 280 °C, with two main

9   decomposition peaks, is due to the decomposition of the grafted polymer brush. From these traces,

10 the average weight percentage of PDMAEMA grafted on silica particles was found to be close to 27 %,

11 which is 24 nm (for calculations, see equation S1 in Supplementary Information), consistent with the

12 expected dry thickness of the brushes generated (from ellipsometry data). In addition, results

13 obtained at different polymerisation times confirmed that the thickness of brushes grown from silica

14 nanoparticles and from silicon wafers were comparable, with a linear increase with polymerisation

15 time (for the reaction time probed, see Supplementary Figure S3). This is a reasonable indicator of

16 control of brush thickness with polymerisation time (although not necessarily implying perfect control

17 of the brush polydispersity). The polybase nature of PDMAEMA brushes was confirmed by *in situ*

18 ellipsometry which gave clear evidence of responsive swelling of the coatings as a function of pH

19 (Supplementary Figure S4). At high pH (above pH 9), PDMAEMA brushes displayed modest swellings

20 (100-200%), consistent with moderately hydrophilic, neutral brushes[29], whilst at lower pH their

21 swelling increased to 200-400%, in good agreement with the expected protonation of DMAEMA

22 repeat units at a pKa of 7.5. In addition, the swelling and collapse behaviour of PDMAEMA brushes

23 displayed a strong hysteresis that was previously attributed, in the case of poly(diethyl aminoethyl

24 methacrylate), to the hindered collapse of brushes upon increase of the pH from acidic conditions[27].

25 Together, these results confirm the reasonable control of PDMAEMA brush growth from silicon and

26 silica substrates and their pH-responsive behaviour.

27

28

29 **Formation of SiO$_2$-g-PDMAEMA/DNA complexes.** To confirm the complexation of DNA by PDMAEMA-

30 functionalised nanoparticles, the interaction of plasmid DNA molecules and polymer brushes (30 nm

31 from silica nanoparticles) in 150 mM NaCl was investigated via dynamic light scattering and

32 electrophoretic light scattering. The plasmid concentration was fixed at 10 μg/mL and the amount of

33 SiO$_2$-g-PDMAEMA nanoparticles introduced was varied to control the N/P ratio of the formed

34 complexes (from 1:1 to 20:1, Figure 2). At low N/P ratios (1:1), plasmid DNA effectively condensed at

11

the surface of PDMAEMA-coated nanoparticles, resulting in a reversal of their zeta potential (from 22.2 mV to −30.1 mV) and a decrease of their hydrodynamic diameter (from 745 to 573 nm, in 150 mM NaCl, Figure 2A). This suggests a partial collapse of the brush structure upon complexation of high levels of DNA and an efficient coverage of the surface of the nanoparticles by plasmid DNA molecules. Indeed, the reversal of the zeta potential suggests an incomplete infiltration of DNA through the brush and a double shell structure resulting in negative charges exposed at the surface of the complexed nanoparticles. Interestingly, this behaviour contrasted with ellipsometry results, which showed an increase in the swollen thickness upon DNA binding (Figure 2B). This is perhaps the result of the lower N/P ratios achieved during in situ ellipsometry experiments, as the DNA concentrations used are expected to be in large excess of the total density of DMAEMA moieties (and therefore amines) present in the brush, due to the low surface area of the interface used compared to complexation of the same amount of DNA by SiO_2-g-PDMAEMA nanoparticles.

At N/P ratios of 5:1 or above, positively charged complexes were formed, in agreement with the expected charge imbalance. This indicates a partial coverage of the particle surfaces by DNA molecules in such conditions and may imply some level of infiltration, resulting in segments of PDMAEMA brushes being exposed at the surface of nanoparticle complexes. Particle sizes also increased significantly at higher N/P ratios, due to aggregation caused by partially infiltrated DNA molecules, able to interact with two neighbouring particles. This phenomenon was particularly pronounced at a moderate N/P ratio of 5:1, compared to 20:1, presumably due to the higher surface density of DNA molecules at a 5:1 charge ratio. Such bimodal evolution of the size of complexes and associated particle aggregation was reported by others for poly(acrylic acid)-functionalised particles complexed by poly(trimethylammonium ethylacrylate) copolymers[30]. However, due to sedimentation of the aggregates formed and their large size (potentially resulting in multiple scattering), the trends observed, rather than the precise hydrodynamic diameters of the aggregates reported, are thought to qualitatively describe the evolution of the complexes generated.

The principal driving force controlling the condensation of DNA is the release of counterions occurring during complexation, mediated by electrostatic interactions between the positively charged groups of the cationic polymer and the negatively charged phosphate groups of DNA molecules[31, 32]. The length of DNA molecules, electrostatic interactions and association with solvent molecules determine their hydrodynamic diameter and the compactness of their conformation[33]. Large electrostatic repulsion between the two strands and the inherent stiffness of the charged helix maintains the elongated coil state of DNA. These electrostatic interactions and the persistence length of DNA chains are, however, reduced as a result of shielding in high salt conditions[34]. Similarly, the conformation of polymer brushes and their density are expected to impact DNA complexation as was observed in the case of

1   other biomacromolecules[35, 36], and should be subjected to substantial reorganisation upon infiltration

2   of PDMAEMA brushes. Overall, our results indicate that, although substantial DNA complexation

3   occurs, DNA infiltration is partial, regardless of the N/P ratio used, and that such surface tethering of

4   DNA molecules controls the colloidal properties of the resulting complexes.

5

6   **In vitro cytotoxicity.** The cytotoxicity of SiO_2-g-PDMAEMA and corresponding DNA complexes was

7   examined next. We studied the impact of N/P charge ratio, DNA complexation and incubation time on

8   the viability of HaCaT cells in serum free medium (Figure 3). The colloidal silica core used in this study

9   is bioinert[37, 38], hence does not influence cytotoxicity greatly whilst cationic brushes are expected to

10   generate some level of cytotoxicity, depending on the concentration of the particles, brush density

11   and length. PDMAEMA itself was shown to display some modest level of cytotoxicity, compared to

12   other cationic polymers[39, 40]. This is thought to be the result of the tertiary amine groups of

13   PDMAEMA's structure, as tertiary amines were found to display lower toxicity than primary and

14   secondary amines[41, 42]. Therefore PDMAEMA, with its tertiary amines, would be expected to display

15   lower cytotoxicity than other coatings with primary or secondary amines and this may be reflected in

16   the relatively low toxicity observed at moderate N/P ratios. At a polymer concentration of 1.5 µg/mL

17   (corresponding to N/P 1:1, with a fixed DNA concentration of 1 µg/mL), cell viability remained

18   comparable to that of the control (cells on tissue culture plastic, Figure 3). As the N/P ratio increased,

19   the cytotoxicity of nanoparticles clearly increased, especially in the absence of DNA complexation,

20   reaching levels as low as 82 % for a polymer concentration of 30 µg/mL (corresponding to a N/P of

21   20:1). DNA is believed to have a protective effect due to the lowering of the surface charge density

22   (especially at low N/P ratios) and the introduction of a steric barrier preventing charged PDMAEMA

23   brushes from direct contact with the cell membrane and preventing its disruption[43, 44]. In addition,

24   cells were found to recover partially from initial cell toxicity as viabilities measured 24 h after

25   transfection were improved compared to 4 h time points. Overall, viabilities measured at N/P ratios

26   of 5/1, 24 h after transfection, were still around 82 %. These toxicity levels are in good agreement with

27   those reported for other cationic polymers (e.g. with fibroblasts COS-7 and MCF-7 cells)[40, 41, 45].

28

29   **Nanoparticle uptake and localisation.** In addition to cytotoxicity, the efficiency of gene expression is

30   controlled by processes involving the uptake of DNA complexes, their intracellular fate and ability to

31   release DNA in the cytoplasm, close to the nucleus[46]. Therefore we next examined the uptake of

32   PDMAEMA-grafted nanoparticles by HaCaT cells. Surface chemistry of the particles is an essential

33   parameter controlling cellular uptake. In that respect, the structure and conformation of PDMAEMA

1 brushes as well as the hydrophilicity of the surface coating of nanoparticles are of particular

2 importance. Generally, it is expected that the cationic polymeric particles would be uptaken more

3 efficiently than neutral or anionic particles, due to electrostatic interaction with the cell membrane,

4 though neutral nanoparticles have been reported to display high cellular uptake[47, 48]. In addition,

5 highly positively charged particles may be further coated by proteins present in cell culture media

6 (from the serum used), which may facilitate cellular uptake in some cases, but can result in particle

7 aggregation. This was previously observed in the case of PMETAC-coated silica nanoparticles[49]. Silica

8 nanoparticles utilised in this study are also believed to enhance uptake by sedimentation to the cell

9 surface[50].

10 To clarify the localisation of DNA-nanoparticle complexes upon incubation with cells, we used

11 fluorescence microscopy to follow the fate of tagged nanoparticles (Figure 4), 4 h after incubation in

12 the culture medium of HaCaT cells (DMEM, 10 % fetal bovine serum). Amino groups were

13 incorporated into the mesoporous silica nanoparticles via co-condensation, in order to serve as

14 coupling sites for the initiator and conjugation sites for the incorporated fluorescent label, FITC.

15 Porous nanoparticles were selected in order to improve the loading of FITC dyes and associated

16 fluorescence of the resulting particles[51]. The impacts of N/P ratios (1, 5 and 10) and complexation of

17 DNA on the localisation of nanoparticles were examined. At low N/P ratios (1:1), very few particles

18 were found associated with cells and it was difficult to determine whether DNA complexation was

19 strongly affecting such localisation. At such N/P ratios, our electrophoretic light scattering data

20 suggested that particles would present a negatively charged surface to cells, hence decreasing their

21 potential uptake (Figure 2). As the N/P ratio increased, nanoparticles were observed to accumulate at

22 increasing densities close to nuclei, in particular at a 10:1 ratio (Figure 4A). The complexation of DNA

23 did not significantly change this trend, although particles were also found in between cells. Confocal

24 laser scanning microscopy was used to investigate the subcellular distribution of particles internalised.

25 Particles are seen to aggregate close to the nuclei, sometimes under or even within nuclear ruffles.

26 The localisation of SiO$_2$-g-PDMAEMA-DNA complexes near the nuclei suggests that particles have

27 bound to the cell surface and internalised and should be able to deliver their payload to transfected

28 cells.

29

30 **Gene delivery with SiO$_2$-g-PDMAEMA nanoparticles.** The transfection efficiency of PDMAEMA brush-

31 grafted silica nanoparticles was determined from the percentage of HaCaT cells expressing EGFP, via

32 fluorescence microscopy. The performance of SiO$_2$-g-PDMAEMA as a transfection agent was evaluated

33 against the commercially available jetPEI® kit, using a plasmid encoding EGFP expression. The

transfection efficiency of SiO$_2$-g-PDMAEMA nanoparticles at N/P ratios 5:1, 10:1 and 15:1 were examined (Figures 5 and Supplementary Figure S5). In addition, the medium (150 mM NaCl solution, PBS or HBS buffer with pH adjusted to 7.4 in all cases) in which the complexes were assembled were altered to investigate the impact of complex formation on transfection. In good agreement with particle localisation results, cell transfection was not significant at a 5:1 N/P ratio. At higher ratios transfection efficiencies increased significantly, in particular at a 15:1 ratio. Higher ratios were not considered due to their higher toxicities. In addition, we found that the type of medium used to assemble the DNA-particle complexes had a strong influence on the overall transfection efficiency. Hence complexes prepared in PBS led to 15.2 % cells expressing EGFP, slightly lower (by 3.6 %) than the efficiencies measured for our positive control (jetPEI) and in agreement with the transfection levels reported for keratinocytes (including HaCaTs) using non-viral vectors[52-55]. In contrast, HBS displayed lower transfection levels at both ratios of 10:1 and 15:1. The buffer used for the formation of complexes therefore seems to have an impact on transfection efficiencies, despite the use of identical media for the actual incubation of cells with the resulting DNA-loaded nanoparticles. In addition, the presence of serum was found to strongly affect overall transfection efficiencies, following a similar trend across the different media used for complex formation, typically leading to a 2-3 fold decrease in the percentage of EGFP expressing cells. Such effect may arise from the binding of serum proteins decreasing the overall surface charge density of the resulting modified complexes.

Our observations that transfections increased significantly above N/P ratios of 5:1 are in good agreement with the literature for free PEI/PDMAEMA polymer chains[56], or free PDMAEMA polymers with a range of molecular weights[15], although some reports indicated transfections already at N/P 5:1 (acetate buffer with 40% sucrose were used for complexation)[57]. Similarly, PDMAEMA-grafted superparamagnetic nanoparticles displayed increased transfection efficiencies at N/P ratios above 10:1[20]. Although the transfection levels observed are encouraging (comparable to those observed for the jetPEI control and those reported in the literature for HaCaT cells[52-55]), they highlight the difficulty to successfully deliver DNA to the nuclei of cells and to see such material being successfully transcribed. Indeed, DNA molecules must dissociate from the condensed complexes sufficiently close to the nucleus, prior to crossing the nuclear envelope (nuclear pores allow molecules prevent molecules or objects above 10 nm from entering), or must preserve their cargo intact until cell division occurs[9, 46]. Hence the regulation of the stability of complexes and DNA dissociation is key and requires a tight control and coordination with molecular transport within the cytoplasm and during the cell cycle[58]. In this respect, cationic polymers allow limited control of such delivery and interactions with cytoplasmic molecules and proteins may significantly alter the stability of DNA-nanoparticle complexes. Following subsequent DNA delivery close to the nucleus, transfection efficiencies are also

1   dependent on the composition of the gene expression system[46]. However, our results indicated that

2   the initial loading and stability of the complexes formed are particularly dependent on the initial

3   medium in which they were assembled. Similar impact of environmental parameters (pH, ionic

4   strength, buffer type) was also reported for the assembly of polyelectrolyte multilayers, analogous to

5   the complexes presently studied[59, 60].

6

7   **Probing DNA-brush interactions via SPR and in situ ellipsometry.** We next explored the origin of the

8   impact of the complexation buffer on transfection efficiencies and proposed it to be the result of

9   changes in interactions between DNA molecules and PDMAEMA brushes. To study such phenomena,

10 we quantified DNA binding to PDMAEMA brushes via surface plasmon resonance (SPR) and in situ

11 ellipsometry (Figure 6 and Supplementary Figure S6). After equilibration of PDMAEMA brushes in the

12 relevant buffers with controlled pH (150 mM NaCl, PBS and HBS, all adjusted at pH 7.4), DNA solutions

13 (1 μg/mL in the corresponding buffer) were injected. SPR traces clearly showed a steady increase in

14 the detected response, corresponding to binding of DNA molecules to the brush-functionalised

15 surface (Figure 6A). This increase was relatively slow, perhaps as a result of the overall low

16 concentration of DNA molecules (compared to other studies of protein binding to brushes) and a slow

17 infiltration of large plasmid DNA molecules. Such interactions were found to be reversible as, when

18 the DNA-adsorbed PDMAEMA surfaces were subsequently exposed to media with a lower pH (5.0),

19 the level of DNA remained unchanged, however, when the pH was raised to 9.0, DNA was released

20 from the brush (Supplementary Figure S7), confirming the role of electrostatic interactions in the

21 binding of nucleic acid molecules. In addition, the level of DNA binding was strongly affected by the

22 type of buffer used and the thickness of the polymer brushes. Hence, whereas DNA binding was not

23 significantly affected by the brush thickness when complexation occurred in 150 mM buffers (Figure

24 6B), it increased 5-fold in PBS when the brush thickness increased from 10 to 30 nm. In comparison,

25 DNA binding in HBS remained very low (46 – 59 ng/cm^2) for both brush thicknesses. Hence our results

26 indicate that DNA binding strongly depends on the complexation buffer as well as brush thickness.

27 To further study interactions between plasmid molecules and polymer brushes, DNA binding was

28 investigated by in situ ellipsometry. These results confirmed the adsorption of DNA molecules in 150

29 mM NaCl solutions, with an average 9 ± 3.2 nm increase in thickness for 10 nm PDMAEMA brushes

30 (dry thickness, the corresponding swollen thickness was 30 nm). In contrast, this increase was not

31 significant for thicker brushes (30 nm dry thickness, 60 nm swollen thickness) in the same buffer,

32 possibly indicating a greater level of infiltration in thicker brushes. In agreement with the SPR data,

33 when DNA solutions in 10 mM HBS were injected, a weaker effect was observed on the resulting

thickness of the complexes 4.4 ± 2.2 nm for 10 nm PDMAEMA brushes. Several processes may play opposite effects on the evolution of the measured wet ellipsometric thickness during DNA binding, as an increase in bound material should result in an increase in thickness, whereas the complexation of cationic brushes by negatively charged DNA could result in the release of water molecules and partial collapse of the complex. Alternatively, DNA infiltration may occur without significant collapse of the complex if water molecules remain strongly associated to the resulting interface. Our results do not support the hypothesis of a collapse of the complex, as the refractive index of the coating did not change significantly prior and after binding and fitting our results with a bilayer or gradient model did not improve the quality of the fits (in all cases mean square errors were found to be below 2.0). In 150 mM NaCl, the refractive index measured decreased from 1.4 to 1.39 upon DNA binding, indicating the adsorption of highly hydrated DNA molecules rather than the collapse of the brush-DNA construct. In HBS, no change in refractive index was observed, although this is not surprising considering the weak binding of DNA to PDMAEMA brushes. Overall, in situ ellipsometry and SPR results imply that DNA molecules strongly bind to PDMAEMA brushes, but that on thin (10 nm) brushes DNA chains are poorly infiltrated and contribute to an increase in the complex thickness, whereas on thicker (30 nm) brushes, more extensive infiltration does not result in significantly increased swollen thicknesses.

Impact of buffer type on brush conformation. We hypothesised that the differences in DNA binding observed in different media were due to changes in PDMAEMA brush conformation, considering that the pH of these media was adjusted to 7.4 in all cases. To test this hypothesis, we studied brush swelling in these different media via in situ ellipsometry and light scattering (Figure 7). We found that although the surface charge of SiO_2-g-PDMEAMA particles remained very similar across the three media tested (ζ potentials of 14, 15 and 20 mV, for 150 mM NaCl, PBS and HBS, respectively, Figure 7A), brush swelling varied significantly. Hence, the hydrodynamic diameter of SiO_2-g-PDMAEMA particles suspended in HBS was found to be considerably higher than that of particles suspended in PBS or 150 mM NaCl media (Figure 7B). Similarly, the swelling of PDMAEMA brushes (30 nm dry) measured in HBS was 290 ± 20 %, whereas that measured in PBS and 150 mM NaCl were 210 ± 10 and 215 ± 10 %, respectively (Figure 7C). Hence, we found a good correlation between brush swelling and the decrease in DNA binding. This is consistent with predictions that propose that the increase in osmotic pressure associated with high brush swelling reduces the adsorption of biomacromolecules[61]. However, the origin of the increased swelling of PDMAEMA brushes in HBS is not clear. Brush swelling is strongly affected by the pH and ionic strength, but as these were kept constant across the three media studied, they cannot account for the changes in conformation observed for HBS. (4-(2-hydroxyethyl)-1-piperazineethanesulfonic acid) (HEPES), the compound controlling the buffering

17

capacity of HBS is a zwitterionic molecule with a piperazine cycle, may be potentially able to bond PDMAEMA brushes (in particular when protonated) and increase the apparent molar mass of the brush repeat units (see Figure 7D). Water molecules would be expected to remain associated with the resulting complexed brushes, due to the high hydrophilicity of the zwitterionic HEPES. In addition, such binding may hinder further binding of negatively charged molecules such as plasmid DNA. Hence, the buffering molecules may interact with polymer brushes and alter both their conformation and interactions with biomacromolecules.

CONCLUSIONS

Our results demonstrate the strong binding of DNA molecules to PDMAEMA brushes and the ability of the resulting complexes to transfect to efficiencies approaching those of the commercial control jetPEI. Beyond the role of parameters recognised to play an important role in transfection in other cationic polymer platforms, such as N/P ratios and the presence of serum during transfection, we identified that the type of medium or buffer used during initial DNA complexation plays an important role in the overall expression level of the corresponding protein. This seems to be an effect mediated by the conformation of polymer brushes during complexation, rather than simply resulting from changes in surface charge density and electrostatic interactions. Hence our results point towards interactions of buffer molecules with polymer brush chains as an important parameter controlling their conformation and associated osmotic pressure. In addition, such buffer-brush interactions may also act as effective competitors of DNA-brush interactions, therefore modulating DNA binding levels and resulting gene transfection. This raises an important question regarding the type of interactions and events that control DNA dissociation from such complexes, upon internalisation. Indeed, our experiments suggest that DNA-PDMAEMA brush complexes should be able to resist the low pH present in the endosome, but the potential role of competitor molecules in transfection culture medium, the endosome or the cytoplasm is not known and the mechanisms controlling the kinetics of DNA dissociation from such complexes not well understood or controlled. This has important implications for design as the control of such kinetics should impact when and where DNA is released, therefore strongly impacting its ability to localise at the nucleus where it can be transcribed to express the targeted protein.

AUTHOR INFORMATION

Corresponding Author.

*E-mail: j.gautrot@qmul.ac.uk.

Notes.

1   The authors declare no competing financial interest.

2

8

9   **SUPPORTING INFORMATION**

10   The Supporting Information is available free of charge on the ACS Publications website at DOI:

11   .Additional experimental results (brush growth kinetics, TGA data, light scattering results at different

12   pH, fluorescence microscopy imaging of transfected cells, SPR data for 10 nm brushes and showing

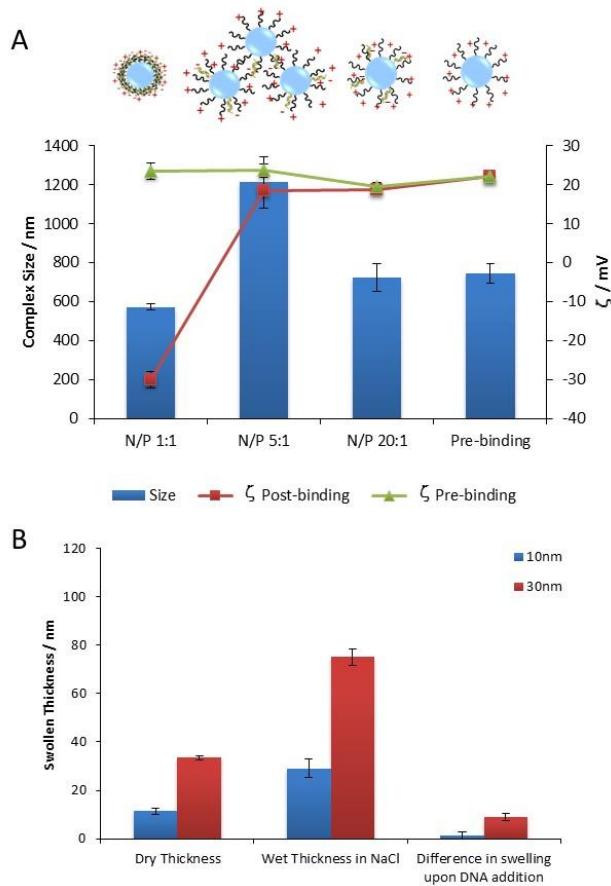13   complex stability upon exposure to media with different pH).

14

15

1
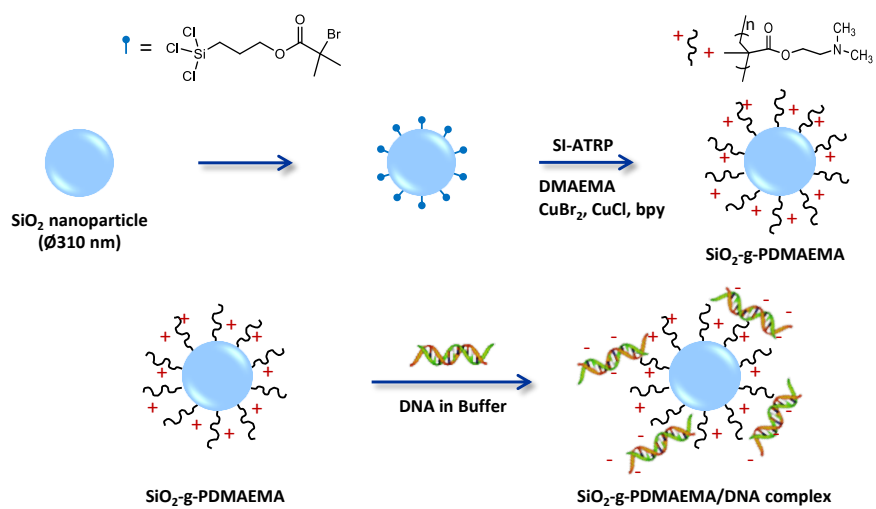
2

3

4 **Figure 1.** Schematic representation of the different steps used for the functionalisation of silica

5 nanoparticle with PDMAEMA brushes and subsequent interaction with DNA molecules (scheme not

6 to scale).

7

Figure 2. Complexation of DNA molecules by PDMAEMA brushes. A, changes in complex size (blue bars) and zeta potential (ζ) before (green triangles) and after (red squares) DNA (10 μg/mL) adsorption to SiO$_2$-g-PDMAEMA nanoparticles (30 nm brushes) at varying N/P ratios, in 150 mM NaCl aqueous solutions. B, effect of DNA addition on the swollen thickness of PDMAEMA brush, grafted from flat silicon substrates at a thickness of either 10 nm (blue) or 30 nm (red) and equilibrated in 150 mM NaCl.
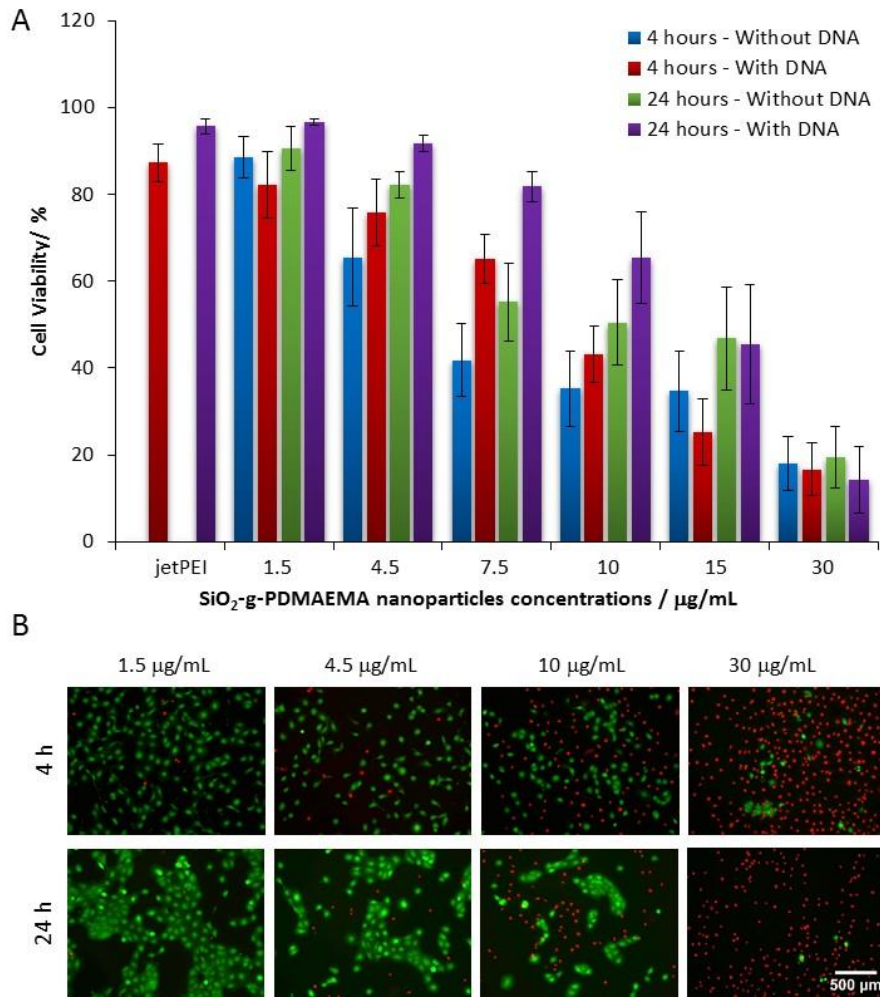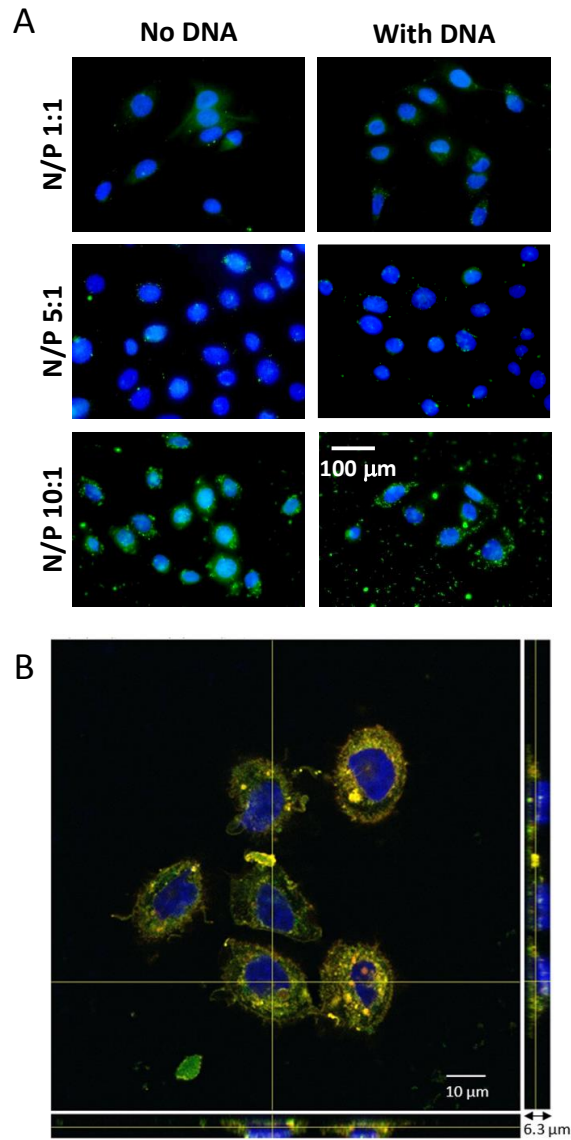
Figure 3. Cytotoxicity of SiO2-g-PDMAEMA nanoparticles, at 4 h and 24 h time points, with and without DNA, assessed on HaCaT cells via live/dead staining assay (A). DNA content was kept constant for all conditions (1 µg/mL). The SiO2-g-PDMAEMA nanoparticles concentrations were in the range of 1.5 to 30 µg/mL. B, corresponding fluorescence microscopy images.

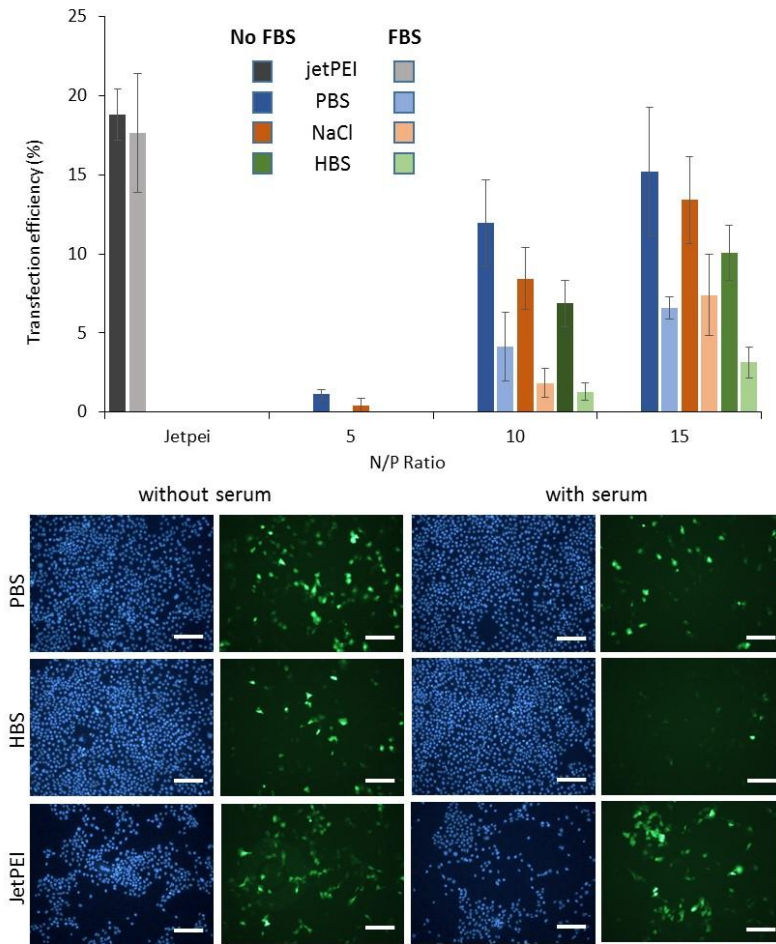**Figure 4.** SiO_2-g-PDMAEMA nanoparticles uptake by HaCaT cells. A. Fluorescence microscopy images capturing cellular uptake of FITC-labelled SiO_2-g-PDMAEMA nanoparticles (green) after 4 h incubation. DNA content was kept constant (1 µg/mL), whereas the amount of SiO_2-g-PDMAEMA nanoparticles was varied to achieve N/P ratios ranging from 1:1 to 10:1. Nuclei (blue) were stained with Hoescht 33342. B. Three-dimensional stacks of confocal images of HaCaTs incubated with FITC-labelled SiO_2-g-PDMAEMA-DNA, with DNA at N/P 10:1.

Figure 5. Transfection efficiency of SiO$_2$-g-PDMAEMA nanoparticles with HaCaTs, measured via the expression of EGFP (A). Complexes were formed using DNA solutions (1 µg/mL) in different buffers (150 mM NaCl, PBS and HBS, pH 7.4) at N/P ratios of 5, 10 and 15. Incubation was carried out for 4 h in media with (+) or without (-) serum (10 % FBS). Experiments were replicated 3 times; * = P < 0.05; ** = P < 0.01; error bars are standard errors. B, corresponding fluorescence microscopy images (full set of images can be found in Supplementary Figure S4).
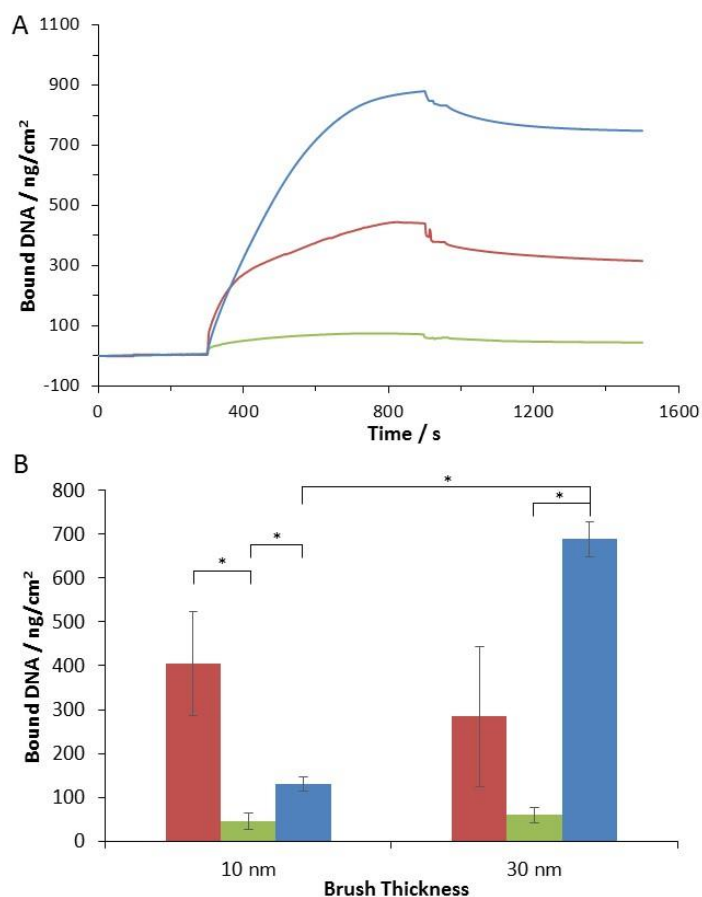
Figure 6. DNA binding to PDMAEMA brushes investigated by SPR. A. Typical SPR traces recorded during the exposure of PDMAEMA brushes (30 nm) to DNA solutions (1 µg/mL). The pH of all buffers (150 mM NaCl, blue line; HBS, green line; PBS, red line) was adjusted to 7.4. B. Summary of the densities of bound DNA at the surface of PDMAEMA brushes (10 and 30 nm) in 150 mM NaCl (blue), 10 mM HBS (green) and PBS (red) solutions. Experiments were carried out in triplicate. * = $p < 0.05$.

1

2
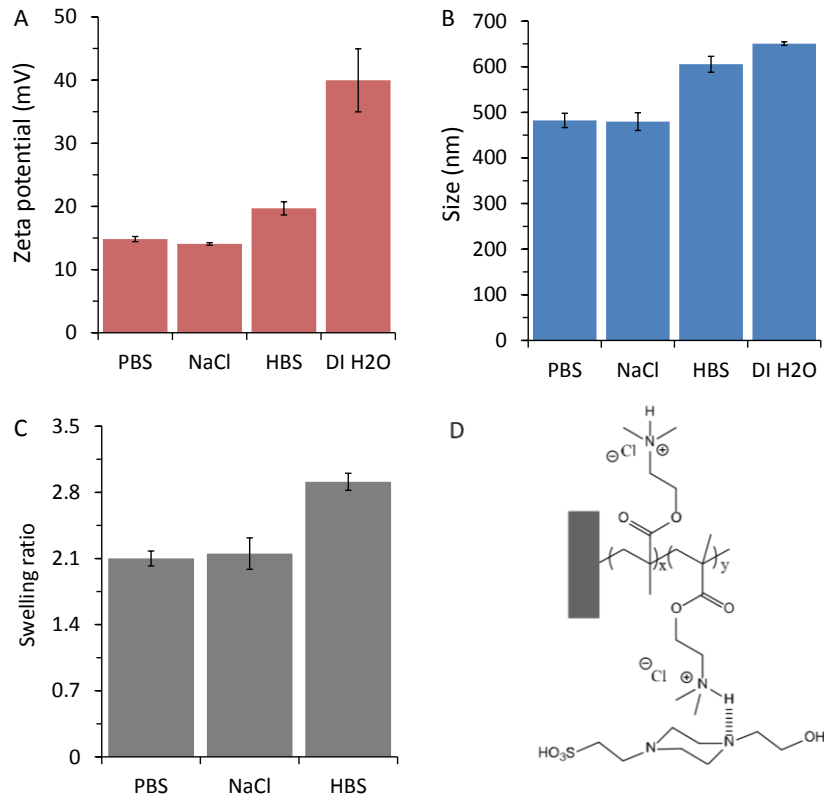
Figure 7. Swelling of PDMAEMA brushes in different media. A. electrophoretic light scattering (zeta potential) and B. dynamic light scattering (size) of SiO_2-g-PDMAEMA particles in PBS, 150 mM NaCl, HBS and DI H_2O. C. Swelling of PDMAEMA brushes (30 nm initial dry thickness) on silicon wafers measured in 150 mM NaCl, PBS and HBS via *in situ* ellipsometry. D. Chemical structure of a PDMAEMA brush (protonated) interacting with a HEPES molecule.

8

9

REFERENCES

(1) Ayres, N., Polymer brushes: Applications in biomaterials and nanotechnology. *Polym. Chem.* **2010,** 1, 769-777.

(2) Barbey, R.; Lavanant, L.; Paripovic, D.; Schuwer, N.; Sugnaux, C.; Tugulu, S.; Klok, H.-A., Polymer brushes via surface-initiated controlled radical polymerization: synthesis, characterization, properties, and applications. *Chem. Rev.* **2009,** 109, 5437-5527.

(3) Chen, T.; Ferris, R.; Zhang, J.; Ducker, R.; Zauscher, S., Stimulus-responsive polymer brushes on surfaces: transduction mechanisms and applications. *Prog. Polym. Sci.* **2010,** 35, 94-112.

(4) Krishnamoorthy, M.; Hakobyan, S.; Ramstedt, M.; Gautrot, J. E., Surface initiated polymer brushes in the biomedical field: applications in membrane science, biosensing, cell culture, regenerative medicine and antibacterial coatings. *Chem. Rev.* **2014,** 114, 10976-11026.

(5) Majewski, A. P.; Stahlschmidt, U.; Jerome, V.; Freitag, R.; Muller, A. H. E.; Schmalz, H., PDMAEMA-Grafted Core-Shell-Corona Particles for Nonviral Gene Delivery and Magnetic Cell Separation. *Biomacromolecules* **2013,** 14, (9), 3081-3090.

(6) Zhang, H. Y.; Lee, M. Y.; Hogg, M. G.; Dordick, J. S.; Sharfstein, S. T., Gene Delivery in Three-Dimensional Cell Cultures by Superparamagnetic Nanoparticles. *Acs Nano* **2010,** 4, (8), 4733-4743.

(7) Pack, D. W.; Hoffman, A. S.; Pun, S.; Stayton, P. S., Design and development of polymers for gene delivery. *Nat. Rev. Drug Discovery* **2005,** 4, 581-593.

(8) Khalil, I. A.; Kogure, K.; Akita, H.; Harashima, H., Uptake pathways and subsequent intracellular trafficking in nonviral gene delivery. *Pharmacol Rev* **2006,** 58, 32-45.

(9) Mintzer, M. A.; Simanek, E. E., Nonviral vectors for gene delivery. *Chem. Rev.* **2009,** 109, 259-302.

(10) Nguyen, D. N.; Green, J. J.; Chan, J. M.; Langer, R.; Anderson, D. G., Polymeric materials for gene delivery and DNA vaccination. *Adv. Mater.* **2009,** 21, 847-867.

(11) Dong, Z.; Wei, H.; Mao, J.; Wang, D.; Yang, M.; Bo, S.; Ji, X., Synthesis and responsive behavior of poly(N,N-dimethylaminoethyl methacrylate) brushes grafted from silica nanoparticles and their quaternized derivatives. *Polymer* **2012,** 53, 2074-2084.

(12) Agarwal, S.; Zhang, Y.; Maji, S.; Greiner, A., PDMAEMA based gene delivery materials. *Mat. Today* **2012,** 15, 388-393.

(13) Arigita, C.; Zuidam, N. J.; Crommelin, D. J.; Hennink, W. E., Association and dissociation characteristics of polymer/DNA complexes used for gene delivery. *Parm. Res.* **1999,** 16, 1534-1541.

(14) Plamper, F. A.; Ruppel, M.; Schmalz, A.; Borisov, O.; Ballauff, M.; Muller, A. H. E., Tuning the thermoresponsive properties of weak polyelectrolytes: aqueous solutions of star-shaped and linear poly(N,N-dimethylaminoethyl methacrylate). *Macromolecules* **2007,** 40, 8361-8366.

(15) Layman, J. M.; Ramirez, S. M.; Green, M. D.; Long, T. E., Influence of polycation molecular weight on poly(2-dimethylaminoethyl methacrylate)-mediated DNA delivery in vitro. *Biomacromolecules* **2009,** 10, 1244-1252.

(16) Lin, S.; Du, F.; Wang, Y.; Ji, S.; Liang, D.; Yu, L.; Li, Z., An acid-labile block copolymer of PDMAEMA and PEG as potential carrier for intelligent gene delivery systems. *Biomacromolecules* **2008,** 9, (1), 109-115.

(17) Dai, F.; Liu, W., Enhanced gene transfection and serum stability of polyplexes by PDMAEMA-polysulfobetaine diblock copolymers. *Biomaterials* **2011,** 32, 628-638.

(18) Xiu, K. M.; Yang, J. J.; Zhao, N. N.; Li, J. S.; Xu, F. J., Multiarm cationic star polymers by atom transfer radical polymerization from β-cyclodextrin cores: influence of arm number and length on gene delivery. *Acta Biomater* **2013,** 9, (1), 4726-4733.

(19) Liu, X.; Yin, H.; Zhang, Z.; Diao, B.; Li, J., Functionalization of lignin through ATRP grafting of poly(2-dimethylaminoethyl methacrylate) for gene delivery. *Colloid Surf. B Biointerfaces* **2015,** 125, 230-237.
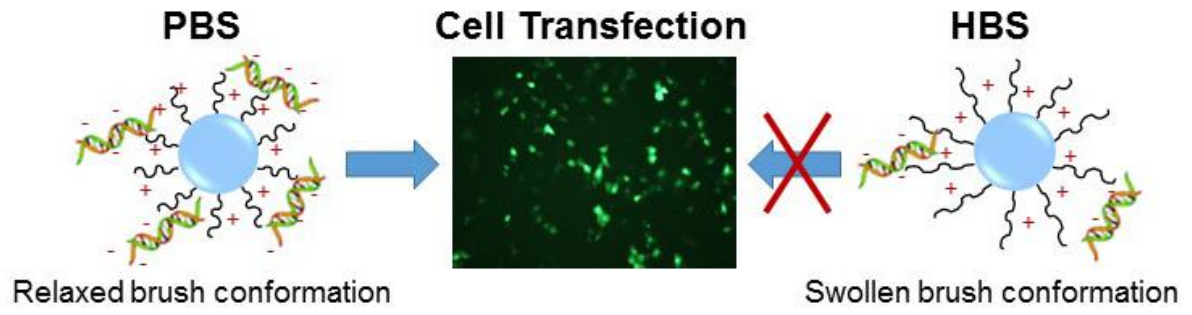
(20) Majewski, A. P.; Stahlschmidt, U.; Jerome, V.; Freitag, R.; Muller, A. H. E.; Schmalz, H., PDMAEMA-grafted core-shell-corona particles for nonviral gene delivery and magnetic cell separation. *Biomacromolecules* **2013,** 14, 3081-3090.

(21) Jones, D. M.; Brown, A. A.; Huck, W. T. S., Surface-Initiated Polymerizations in Aqueous Media: Effect of Initiator Density. *Langmuir* **2002,** 18, (4), 1265-1269.

(22) Jonas, A. M.; Glinel, K.; Oren, R.; Nysten, B.; Huck, W. T. S., Thermo-responsive polymer brushes with tunable collapse temperatures in the physiological range. *Macromolecules* **2007,** 40, 4403-4405.

(23) Husseman, M.; Malmstrom, E.; McNamara, M.; Mate, M.; Mecerreyes, D.; Benoit, D. G.; Hedrick, J. L.; Mansky, P.; Huang, E.; Russell, T. P.; Hawker, C. J., Controlled synthesis of polymer brushes by "living" free radical polymerization techiniques. *Macromolecules* **1999,** 32, 1424-1431.

(24) Desai, D.; Sen Karaman, D.; Prabhakar, N.; Tadayon, S.; Duchanoy, A.; Toivola, D. M.; Rajput, S.; Nareoja, T.; Rosenholm, J. M., Design considerations for mesoporous silica nanoparticulate systems in facilitating biomedical applications. *Mesoporous Biomater.* **2014,** 1, 16-43.

(25) Tan, K. Y.; Gautrot, J. E.; Huck, W. T. S., Formation of pickering emulsions using ion-specific responsive colloids. *Langmuir* **2011,** 27, 1251-1259.

(26) Tan, K. Y.; Gautrot, J. E.; Huck, W. T. S., Island brushes to control adhesion of water in oil droplets on planar surfaces. *Soft Matter* **2011,** 7, 7013-7020.

(27) Willott, J. D.; Murdoch, T. J.; Humphreys, B. A.; Edmondson, S.; Webber, G. B.; Wanless, E. J., Critical salt effects in the swelling behavior of a weak polybasic brush. *Langmuir* **2014,** 30, (7), 1827-1836.

(28) Cheesman, B. T.; Willott, J. D.; Webber, G. B.; Edmondson, S.; Wanless, E. J., pH-Responsive Brush-Modified Silica Hybrids Synthesized by Surface-Initiated ARGET ATRP. *ACS Macro Letters* **2012,** 1, (10), 1161-1165.

(29) Hackett, A. J.; Malmström, J.; Molino, P. J.; Gautrot, J. E.; Zhang, H.; Higgins, M. J.; Wallace, G. G.; Williams, D. E.; Travas-Sejdic, J., Conductive surfaces with dynamic switching in response to temperature and salt. *J. Mater. Chem. B* **2015,** 3, 9285-9294.

(30) Fresnais, J.; Lavelle, C.; Berret, J. F., Nanoparticle Aggregation Controlled by Desalting Kinetics. *The Journal of Physical Chemistry C* **2009,** 113, (37), 16371-16379.

(31) Vijayanathan, V.; Thomas, T., DNA Nanoparticles and development of DNA delivery vehicles for gene therapy. *Biochem.* **2002,** 41, 14085-14094.

(32) Howard, K. A.; Dash, P. R.; Read, M. L.; Ward, K.; Tomkins, L. M.; Nazarova, O.; Ilbrich, K.; Seymour, L. W., Influence of hydrophilicity of cationic polymers on the biophysical properties of polyelectrolyte complexes formed by self-assembly with DNA. *Biochim. Biophys. Acta* **2000,** 1475, 245-255.

(33) Jorge, A. F.; Dias, R. S.; Pereira, J. C.; Pais, A. A. A. C., DNA condensation by pH-responsive polycations. *Biomacromolecules* **2010,** 11, (9), 2399-2406.

(34) Baumann, C. G.; Smith, S. B.; Bloomfield, V. A.; Bustamante, C., Ionic effects on the elasticity of single DNA molecules. *Proc. Natl. Acad. Sci.* **1997,** 94, 6185-6190.

(35) de Vos, W. M.; Biesheuvel, P. M.; de Keizer, A.; Kleijn, J. M.; Cohen Stuart, M. A., Adsorption of the protein bovine serum albumin in a planar poly(acrylic acid) brush layer as measured by optical reflectometry. *Langmuir* **2008,** 24, 6575-6584.

(36) Wang, S.; Kaimin, C.; Li, L.; Xuhong, G., Binding between proteins and cationic spherical polyelectrolyte brushes: effect of pH, ionic strength and stoichiometry. *Biomacromolecules* **2013,** 14, 818-827.

(37) Kneuer, C.; Sameti, M.; Bakowsky, U.; Schiestel, T.; Schirra, H.; Schmidt, H.; Lehr, C. M., A nonviral DNA delivery system based on surface modified silica-nanoparticles can efficiently transfect cells in vitro. *Bioconj. Chem.* **2000,** 11, 926-932.

(38) Barbe, C.; Bartlett, J.; Kong, L.; Finnie, K.; Lin, H. Q.; Larkin, M.; Calleja, S.; Bush, A.; Calleja, G., Silica particles: a novel drug delivery system. *Adv. Mater.* **2004,** 16, 1959-1966.

(39) van de Wetering, P.; Cherng, J.-Y.; Talsma, H.; Hennink, W. E., Relation between transfection efficiency and cytotoxicity of poly(2-dimethylaminoethyl methacrylate)/plasmid complexes. *J. Control. Release* **1997,** 49, 59-69.

(40) Cai, J.; Yue, Y.; Rui, D.; Zhang, Y.; Liu, S.; Wu, C., Effect of chain length on cytotoxicity and endocytosis of cationic polymers. *Macromolecules* **2011,** 44, (7), 2050-2057.

(41) Fischer, D., Y; Ahlemeyer, B.; Krieglstein, J.; Kissel, T., In vitro cytotoxicity testing of polycations: influence of polymer structure on cell viability and hemolysis. *Biomaterials* **2003,** 24, 1121-1131.

(42) Ferruti, P.; Knobloch, S.; Ranucci, E.; Duncan, R.; Gianasi, E., A novel modification of poly(L-Lysine) leading to a soluble cationic polymer with reduced toxicity and with potential as a transfection agent. *Macromol. Chem. Phys.* **1998,** 199, 2565-2575.

(43) Boussif, O.; Lezoualc'h, F.; Zanta, M.; Mergny, M. D.; Scherman, D.; Demeneix, B.; Behr, J. P., A versatile vector for gene and oligonucleotide transfer into cells in culture and in vivo: polyethylenimine. *Proc. Natl. Acad. Sci.* **1995,** 92, 7297-7301.

(44) Cherng, J. Y.; van de Wetering, P.; Talsma, H.; Crommelin, D. J.; Hennink, W. E., Effect of size and serum proteins on transfection efficiency of poly ((2-dimethylamino)ethyl methacrylate)-plasmid nanoparticles. *Pharmacol Res* **1996,** 13, 1038-1042.

(45) Kean, T.; Roth, S.; Thanou, M., Trimethylated chitosans as non-viral gene delivery vectors: cytotoxicity and transfection efficiency. *J. Control. Release* **2005,** 103, 643-653.

(46) Luo, D.; Saltzman, W. M., Synthetic DNA delivery systems. *Nat. Biotechnol.* **2000,** 18, 33-37.

(47) Freese, C.; Gibson, M. I.; Klok, H. A.; Unger, R. E.; Kirkpatrick, C. J., Size- and coating-dependent uptake of polymer-coated gold nanoparticles in primary human dermal microvascular endothelial cells. *Biomacromolecules* **2012,** 13, 1533-1543.

(48) Hauck, T. S.; Ghazani, A. A.; Chan, W. C., Assessing the effect of surface chemistry on gold nanorod uptake, toxicity, and gene expression in mammalian cells. *Small* **2008,** 4, 153-159.

(49) Tan, K. Y.; Lin, H.; Ramstedt, M.; Watt, F. M.; Huck, W. T. S.; Gautrot, J. E., Decoupling geometrical and chemical cues directing epidermal stem cell fate on polymer brush-based cell micro-patterns. *Integr. Biol.* **2013,** 5, 899-910.

(50) Luo, D.; Saltzman, W. M., Enhancement of transfection by physical concentration of DNA at the cell surface. *Nat. Biotechnol.* **2000,** 18, 893-895.

(51) Gulin-Sarfraz, T.; Sarfraz, J.; Sen Karaman, D.; Zhang, J.; Oetken-Lindholm, C.; Duchanoy, A.; Rosenholm, J. M.; Abankwa, D., FRET-reporter nanoparticles to monitor redox-induced intracellular delivery of active compounds. *RSC Adv.* **2014,** 4, 16429-16437.

(52) Deyrieux, A. F.; Wilson, V. G., In vitro culture conditions to study kerationcyte differentiation using the HaCaT cell line. *Cytotechnology* **2007,** 54, 77-83.

(53) Huber, M.; Limat, A.; Wagner, E.; Hohl, D., Efficient in vitro transfection of human keratinocytes with an adenovirus-enhanced receptor-mediated system. *J. Invest. Dermatol.* **2000,** 114, (4), 661-666.

(54) Nead, M. A.; McCance, D. J., Poly-L-ornithine-mediated transfection of human keratinocytes. *J. Invest. Dermatol.* **1995,** 105, (5), 668-671.

(55) Zare, S.; Zarei, M. A.; Ghadimi, T.; Fathi, F.; Jalili, A.; Hakhamaneshi, S., Isolation, cultivation and transfection of human keratinocytes. *Cell Biol. Int.* **2014,** 38, 441-451.

(56) Schallon, A.; Jérôme, V.; Walther, A.; Synatschke, C. V.; Müller, A. H. E.; Freitag, R., Performance of three PDMAEMA-based polycation architectures as gene delivery agents in comparison to linear and branched PEI. *React. Funct. Polym.* **2010,** 70, 1-10.

(57) Verbaan, F. J.; Klein Klouwenberg, P.; van Steenis, J. H.; Snel, C. J.; Boerman, O.; Hennink, W. E.; Storm, G., Application of poly(2-(dimethylamino)ethyl methacrylate)-based polyplexes for gene transfer into human ovarian carcinoma cells. *Int. J. Pharm.* **2005,** 304, 185-192.

(58) Parhamifar, L.; Larsen, A. K.; Hunter, A. C.; Andresen, T. L.; Moghimi, S. M., Polycation cytotoxicity: a delicate matter for nucleic acid therapy - focus on polyethylenimine. *Soft Matter* **2010,** 6, 4001.

(59) Bertrand, P.; Jonas, A.; Laschewsky, A.; Legras, R., Ultrathin polymer coatings by complexation of polyelectrolytes at interfaces: suitable materials, structure and properties. *Macromol. Rapid Commun.* **2000,** 21, 319-348.

(60) Guzey, D.; McClements, D. J., Formation, stability and properties of multilayer emulsions for application in the food industry. *Adv. Colloid. Interf. Sci.* **2006,** 128-130, 227-248.

(61) Halperin, A.; Kroger, M., Collapse of thermoresponsive brushes and the tuning of protein adsorption. *Macromolecules* **2011,** 44, 6986-7005.

PBS   Cell Transfection   HBS

Relaxed brush conformation   Swollen brush conformation

1

2

3   **Table of Content Figure**